

## Magnetically Controlled Mass Loss from Exoplanets

Fred C. Adams<sup>1,2</sup> and James E. Owen<sup>3</sup>

<sup>1</sup>*Michigan Center for Theoretical Physics  
Physics Department, University of Michigan, Ann Arbor, MI 48109*

<sup>2</sup>*Astronomy Department, University of Michigan, Ann Arbor, MI 48109*

<sup>3</sup>*Canadian Institute for Theoretical Astrophysics  
University of Toronto, 60 St. George Street, Toronto, Ontario, Canada*

**Abstract.** Hot Jupiters can experience mass loss driven by heating from UV radiation from their host stars, and this flow is often controlled by magnetic fields. More specifically, near the planetary surface, the magnetic pressure dominates the ram pressure of the outflow by several orders of magnitude. After leaving the vicinity of the planet, the flow must connect onto the background environment provided by the stellar wind and the stellar magnetic field. This contribution considers magnetically controlled planetary outflows and extends previous work by comparing two different geometries for the background magnetic field provided by the star. In the first case, stellar field is assumed to retain the form of a dipole, which is anti-aligned with the dipole field of the planet. In the second case, the stellar outflow opens up the stellar magnetic field structure so that the background field at the location of the planet is perpendicular to the planetary dipole. Using numerical simulations, we consider the launch of the planetary wind with these field configurations.

### 1. Introduction

Thousands of alien worlds have now been discovered. As the galaxy-wide planetary census continues to grow, we can probe their physical properties, orbital dynamics, chemical composition, and even their weather. Although they are not the most common planets, Hot Jupiters with orbital periods of 2 – 5 days play a vital role: Almost everything that is currently known about the physical — as opposed to orbital — properties of extrasolar planets has been obtained from the subset of these planets that are observed to transit bright stars.

The galactic inventory of Hot Jupiters has increased steadily. Nearly 600 of the exoplanets discovered to date orbit their stars with periods of 10 days or less. Conventional wisdom (Lissauer & Stevenson, 2007) holds that these planets formed at larger distances from their parent stars and subsequently moved inward through the action of disk migration (Lin et al., 1996; Papaloizou & Terquem, 2006), planet-planet scattering (Rasio & Ford, 1996; Moorhead & Adams, 2005), or Kozai cycles with tidal friction (Eggleton et al., 1998; Wu & Murray, 2003; Fabrycky & Tremaine, 2007). After migration, the planets become stranded at small semimajor axes ( $a \lesssim 0.1$  AU).

After the planets reach their inner orbits, they are subjected to intense heating from the central star. This heating, which is most effective for UV photons, can drive photo-evaporative flows from the planetary surfaces and also generates ionization levels high enough so that MHD effects play a role. In extreme cases, planetary mass loss can affect both the final masses and densities of the planets. A good example is provided by the observed Roche lobe overflow from WASP-12b. Planets of lower mass are influenced to a greater degree (Owen & Wu, 2013). Moreover, outflows can be observable even if their effect on the final mass is modest, and can provide important information about planetary properties. Mass loss from extrasolar planets has already been observed for two transiting planets associated with bright stars: HD209458b (Vidal-Madjar et al., 2003) and HD189733b (Lecavelier des Etangs et al., 2010).

Theoretical calculations of mass loss from extrasolar planets have shown a steady progression. Pioneering models of outflows from these planetary bodies have been constructed (Lammer et al., 2003; Baraffe et al., 2004, 2006) and indicate that substantial mass loss can take place. These studies primarily use energy-limited outflow models (Waston et al., 1981), in conjunction with physically motivated scaling laws, and predict a range of outflow rates for given planetary masses and external UV fluxes. The next generation of calculations considered refined treatments of the chemistry, photoionization, and recombination (Yelle, 2004; Garcia-Munoz, 2007) as well as including the effects of tidal enhancement (Murray-Clay et al., 2009). Next, two-dimensional effects (allowing non-spherical geometry) in planetary winds were considered (Stone & Proga, 2009) and indicate that the mass loss rates can be less than those in the spherical limit. Alternative explanations of the observations have also been put forth, wherein the inferred excess material is due to a confined exosphere (Trammell et al., 2011) or a mass transfer stream (Lai et al., 2010). However, the observations show high velocity signatures, which indicate winds or outflows, rather than static structures (see also Holmström et al. 2008). For completeness, we also note that interactions between close planets and stellar magnetospheres can produce interesting observable signatures (Shkolnik et al., 2005, 2008; Lanza, 2008, 2009).

Magnetic fields with moderate strength ( $B \gtrsim 0.3$  gauss) are sufficient to completely dominate the ram pressure of the winds and thereby control the flow. In spite of this dominance, however, magnetic fields are generally ignored in models of planetary winds. The first studies including magnetic fields considered analytic and semi-analytic treatments of flow (Adams, 2011; Trammell et al., 2011), and found that not all field lines are active; this reduction leads to suppression of the mass loss rate. Subsequent numerical studies confirm this finding (Trammell et al., 2014; Owen & Adams, 2014), and indicate that the the flow is magnetically controlled even for the highest expected UV fluxes (with moderate field strengths) and that outflow from the night side of the planet is also suppressed. The aforementioned numerical studies consider the magnetic field of the background star to be anti-aligned with the planetary dipole (Owen & Adams, 2014) or do not include it (Trammell et al., 2014). Nonetheless, the background field geometry can play an important role. This contribution compares two choices for the background magnetic field provided by the star. In the first case, we consider the field to be anti-aligned (as in Owen & Adams 2014). In the second case we assume that the stellar wind is strong enough to open up the stellar magnetic field into a split-monopole configuration; as a result, the background field at the location of the planet is perpendicular to the planetary dipole.

## 2. Basics

We start by outlining the basic physics of the problem: If the UV flux from the star provides sufficient heating, so that the sound speed at the planetary surface is greater than the depth of the potential well,  $a_S^2 > GM_P/R_P$ , then mass loss occurs without suppression. The outflow rate is then roughly given by  $\dot{M} = 4\pi R_P^2 a_S \rho$ , where  $\rho$  is the gas density at the radius  $R_P$ . In practice, however, the sound speed is smaller than this benchmark value. For typical systems, the sound speed  $a_S \approx 10$  km/s and the escape speed is  $\sim 50 - 60$  km/s, so that  $a_S^2 < GM_P/R_P$  and outflow can occur only at larger radii, above the planetary “surface” at  $R_P$ . At these larger radii, the gas temperatures are higher because the stellar UV flux is less attenuated, and the gravitational potential well is shallower. Both of these trends act to increase mass loss. However, the gas density decreases rapidly with radius (above the planetary surface) and this lower density leads to a lower mass loss rate. As a result, outflow rates  $\dot{M}$  are determined by a delicate balance between the UV heating rate and the depth of the gravitational potential well at the launching point. To leading order, we can estimate the expected outflow rate as follows: If the outflow is limited by the rate at which the gas gains energy from the stellar UV flux, the mechanical luminosity of the outflow must balance the rate of energy deposition,

$$\frac{GM_P \dot{M}}{R_P} = \varepsilon F_{UV} \pi R^2, \quad (1)$$

where  $\varepsilon$  is an efficiency factor and  $R = \alpha R_P$  determines the area over which energy is absorbed. The mass outflow rate is thus given by

$$\dot{M} = \varepsilon \alpha^2 \pi \frac{R_P^3 F_{UV}}{(GM_P)}. \quad (2)$$

For a Jovian planet in a 4-day orbit about a Sun-like star, we expect  $F_{UV} \approx 450$  erg cm<sup>-2</sup> s<sup>-1</sup>, and the expected mass outflow rate  $\dot{M} \sim 10^{10}$  g/s. This value is in rough agreement with the inferred outflow rates for the planets HD209458b and HD189733b, indicating that planetary mass loss driven by UV heating is plausible. However, the outflow process is more complicated than this idealized picture.

The defining feature of this work is the inclusion of magnetic fields, which are strong enough to influence the flow (Adams, 2011; Trammell et al., 2011). These fields arise from both the star and the planet. When the outflow follows the magnetic field lines, the flow geometry is set by the field structure, which can be quite complicated. In particular, the outflows depart significantly from spherical symmetry and previous (primarily spherical) wind models are not applicable. In spite of this complication, the outflow problem can be reduced to one flow dimension by constructing a new coordinate system where one coordinate follows the magnetic field lines. This approach allows for the outflow properties and the passage through the sonic points to be determined semi-analytically (Adams, 2011; Adams & Gregory, 2012).

To leading order, the stellar and the planetary magnetic fields are expected to have dipole forms. Typical field strengths on the surfaces of stars that host Hot Jupiters are measured to be  $B_* \sim 40$  G (e.g., for HD189733; Fares et al. 2010).

The surface field strength for the planets are expected to be  $B_P \sim 10$  G (with a factor of  $\sim 10$  variation; see Batygin & Stevenson 2010 and references therein). Near the planet, we expect that its dipole field dominates, and the stellar field provides a background field of nearly constant strength and direction (as seen from the scale of the planet). The simplest case where the background field of the star is anti-aligned with planetary dipole can be addressed analytically. An important complication arises because the dipole field of the star can be opened up by the stellar wind, so that the background field (from the star) becomes nearly radial (split monopole configuration). This effect can be modeled via potential fields with multiple components (Adams, 2011; Adams & Gregory, 2012), or by introducing a source surface (Gregory et al., 2010; Gregory, 2011). In either case, the stellar field transitions from a dipole to a split monopole configuration at a (relatively) well-defined radius  $r_S$ . Observations of star-planet interactions are starting to put constraints on field geometries, but planetary orbits (with 4 day periods and  $a \sim 0.05$  AU) could lie on either side of the transition radius  $r_S$  (Fares et al., 2010). In addition, if the dipole is highly tilted with respect to the orbital plane, stellar field can be essentially radial at the position of the planet, even if the field lines are not opened up. As a result, planetary outflows are expected to experience a wide range of possibilities for the background magnetic configurations provided by their host stars.

In order for the magnetic field to influence the outflow, the plasma must be well-coupled to the field, which requires the cyclotron frequency  $\omega_C$  to be larger than the collision frequency  $\Gamma_C$ . Straightforward calculations indicate that  $\omega_C \gg \Gamma_C$  from the planetary surface all the way out to  $r \sim 10^4 R_P$ , so that the outflow will indeed be well-coupled to the magnetic field (Adams, 2011; Trammell et al., 2011). Another necessary condition for the magnetic field to guide the outflow is that the magnetic pressure must be larger than the ram pressure of the flow, i.e.,  $B^2/8\pi \gg \rho v^2$ . The ram pressure is given by the outflow rate ( $\dot{M} \sim 10^{10}$  g/s) in conjunction with the flow speed ( $v \sim a_S \sim 10$  km/s). The magnetic field can be approximated as a dipole, with surface field strength comparable to Jupiter ( $B_P \approx 4$  G) and the usual spatial dependence  $B \propto r^{-3}$ . For typical parameters, we find that the magnetic pressure is larger than the ram pressure of the outflow by a factor of  $\sim 10^4$  at the sonic surface and by a factor of  $\sim 10^6$  at the planetary surface. These considerations show that the magnetic field is well-coupled and that *the outflow must be magnetically controlled*.

For this work, we consider the magnetic field of the planet to be a dipole oriented in the  $\hat{z}$  direction. The outflow takes place on the spatial scale of the planetary radius  $R_P$ , which is much smaller than the stellar radius  $R_*$  and the orbital scale  $a$ . As a result, for purposes of studying the launch of the outflow, the background magnetic field of the star can be considered as a uniform field with a constant direction. The total field thus can be written

$$\mathbf{B} = B_P \left[ \xi^{-3} (\cos \theta \hat{r} - \hat{z}) + \beta \hat{s} \right], \quad (3)$$

where  $B_P$  is the surface field strength of the planet and we have defined  $\xi \equiv r/R_P$ . The parameter  $\beta$  sets the strength of the background stellar field (evaluated at the orbit of the planet) and  $\hat{s}$  defines its direction (here we take either  $\hat{s} = \hat{z}$  or  $\hat{s} = \hat{x}$ ). Since both the star and planet are expected to have surface field strengths of a few gauss, and since Hot Jupiters orbit at distances  $a \sim 10R_*$ , we expect the parameter  $\beta \sim 10^{-3}$ .

### 3. Numerical Calculations

In order to study magnetically controlled outflow from planets, as outlined in the previous section, we perform simulations of the outflow problem (Owen & Adams, 2014). In this numerical treatment, we solve the Radiation-MHD problem in the ideal MHD limit, i.e., the magnetic structure is allowed to respond to the flow. These numerical calculations are carried out using a modified version of the ZEUS-MP MHD code (Stone & Norman, 1992a,b; Hayes et al., 2006). In addition to the standard ideal-MHD equations, we also solve for the ionization fraction in the flow and solve the radiative transfer problem for incoming ionizing photons (see Owen & Adams 2014 for further detail).

One constraint on this approach is that we assume that the recombination time is short compared to the flow time and that the mean-free path of the ionizing photons is short compared to the flow length-scale at the ionization front. These assumptions are valid only for the largest UV fluxes ( $F_{UV} \gtrsim 10^5 \text{ erg s}^{-1}$ , values appropriate for young Sun-like stars), so that the gas is close to radiative-recombination equilibrium. In this regime, the thermal structure in the flow is simplified, where ionized gas is nearly isothermal at  $T = 10^4 \text{ K}$  and neutral gas is nearly isothermal at  $T = 10^3 \text{ K}$ . Even with such high UV fluxes, the simulations show that the outflows are safely controlled by the magnetic fields (Owen & Adams, 2014). Moreover, if the outflow is magnetically dominated at high fluxes, it will also be magnetically dominated at lower fluxes since the mass-loss rate increases with increasing flux.

The calculations are performed using a 2D spherical grid  $(r, \theta)$  with the assumption of azimuthal symmetry; the inner boundary is set at  $r = 10^{10} \text{ cm}$  and the outer boundary at  $r = 1.5 \times 10^{11} \text{ cm}$  ( $R_P \leq r \leq 15R_P$ ). For comparison, the outflow passes through the sonic point when the radius  $r \approx 3R_P$ . The radial grid is non-uniform with size  $N_r = 128$ , where the resolution at the inner boundary is sufficient to resolve the scale height of the underlying atmosphere. In the angular direction we use a uniform grid with 64 cells per quadrant. At the inner boundary we apply fixed boundary conditions where the density  $\rho = 10^{-11} \text{ g cm}^{-3}$ , the temperature  $T = 10^3 \text{ K}$ , the magnetic field is a dipole with strength  $B_P$ , and the ionization fraction  $X = 10^{-5}$ . On the outer boundary we adopt outflow boundary conditions, but include the contribution from the background stellar field (controlled by the parameter  $\beta$ ; see equation [3]). Finally, on the angular boundaries we adopt the appropriate symmetry boundary conditions (see Owen & Adams 2014 for further detail). In order to isolate the effects of the magnetic field, we neglect the small contributions from planetary rotation and the stellar gravitational field (see Trammell et al. 2014).

Previous simulations have shown that the outflow is highly suppressed from the night side of the planet (Owen & Adams, 2014); as a result, this work considers only the day side. This previous work carried out a survey of the relevant parameter space, with variations in the field strength ratio  $\beta$ , the planetary surface magnetic field strengths  $B_P$ , and the UV flux  $F_{UV}$  from the host star. All of these simulations assume that the background stellar field is anti-aligned with the dipole of the planet. Representative results from these simulations are shown in Figure 1, which presents the outflow patterns and magnetic field configurations for planets subjected to intense UV radiation fields with flux  $F_{UV} = 10^6 \text{ erg s}^{-1} \text{ cm}^{-2}$ . The figures shows the results obtained for four planetary magnetic field strengths ( $B_P = 0.5, 1, 4.0$  and  $10$  gauss from top to bottom) and two values

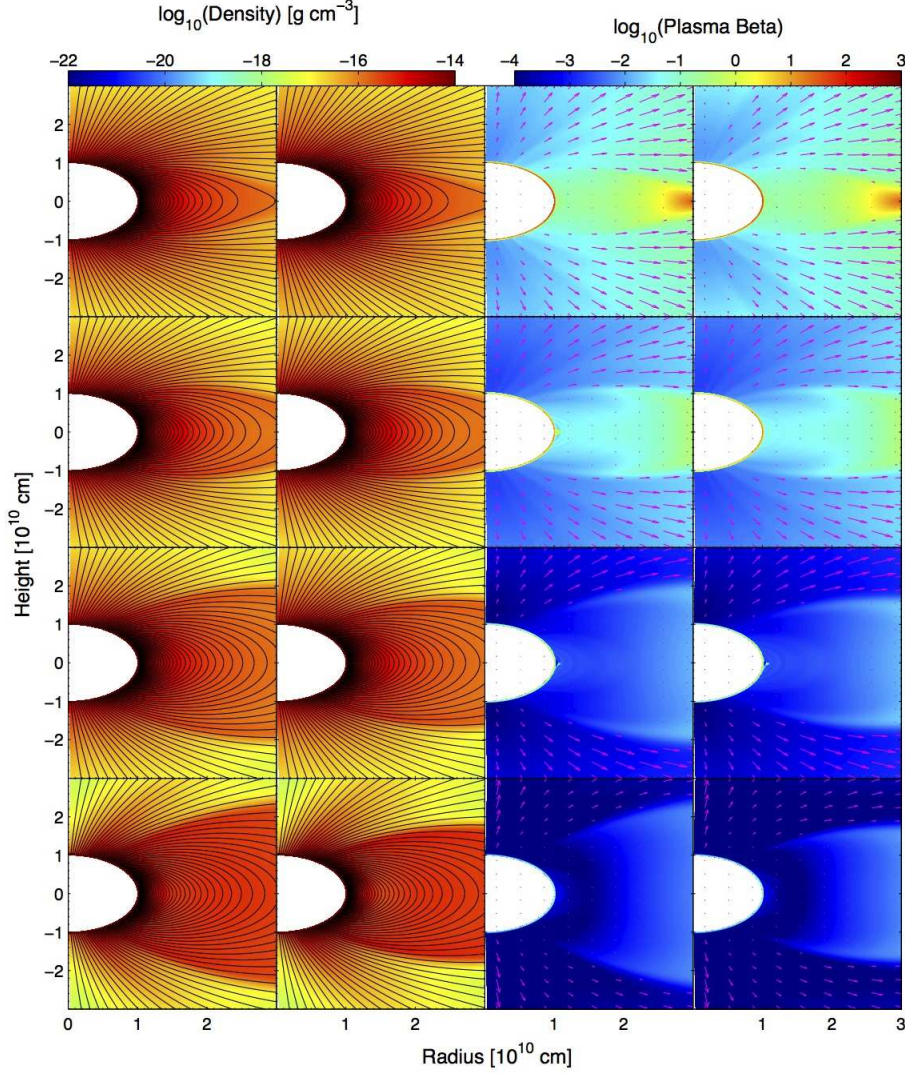


Figure 1.: *Flow topologies for a subset of parameter space where both the stellar background field and the magnetic dipole of the planet point in the  $\hat{z}$  direction. The rows represent planetary magnetic field strengths from  $B_P = 0.5$  (top) to 10 (bottom) gauss. The first two columns show the density and magnetic field topology, where  $\beta = 0$  ( $\beta = 3 \times 10^{-3}$ ) for the first (second) column. The final two columns show the plasma beta and velocity structure, where  $\beta = 0$  ( $\beta = 3 \times 10^{-3}$ ) for the third (fourth) column. The panels show only the inner regions of the simulations (which extend out to 15 planetary radii). The star is located along the positive  $x$ -axis.*

of the stellar magnetic field parameter ( $\beta = 0$  and  $3 \times 10^{-3}$  from left to right). The first two columns show density and magnetic field topology; the second two columns show the plasma beta and velocity structure.

The results shown in Figure 1 show several trends. As the planetary field strength  $B_P$  decreases, the evaporative flow is able to open up an increasing number of magnetic field lines and thereby produce higher mass outflow rates. As the background field strength parameter  $\beta$  increases, a similar effects takes place as the background field opens up more field lines and thereby allows mass loss to take place from a larger fraction of the planetary surface (see Adams 2011 for an analytic treatment of this latter effect). Notice that for relatively weak planetary fields,  $B_P \lesssim 1$  gauss, the opening of field lines is primarily due to the outflow itself; for stronger fields,  $B_P \gtrsim 1$  gauss, the number of opening field lines depends strongly on the strength (and also topology) of the background stellar field. We emphasize that these results were obtained for large stellar UV fluxes. For smaller values of  $F_{UV}$ , the background stellar field will dominate the process of field line opening for smaller surface field strengths  $B_P$ .

For all of the simulations with magnetic fields included, we find that the mass outflow rates are smaller than those obtained in the absence of fields. This suppression is significant, approximately an order of magnitude, although the ratio varies with the other parameters of the problem (see Owen & Adams 2014). Finally, we note that even for the highest possible UV fluxes, which drive the most energetic outflows, the flow is magnetically controlled. Although the numerical treatment allows for the magnetic field lines to evolve in response to the fluid motions, the magnetic field configurations do not change significantly from their starting geometries over the course of the simulations.

For comparison, Figure 2 shows the result from an analogous numerical simulation, where the background stellar field has a different direction (and is not aligned with the dipole of the planet). The star is assumed to have a split-monopole configuration, as expected when the stellar wind is strong enough to break open the stellar field lines. From the small-scale viewpoint of the planet, the background stellar field is uniform, but points in the  $\hat{x}$  direction (radially towards the star). Results are shown for the positive- $x$ , positive- $z$  quadrant; since the mid-plane boundary conditions assume that the star has a split monopole field, the density structure of the flow has mid-plane reflection symmetry. Although the magnetic fields are relatively weak (with  $B_P = 0.5$  gauss and  $\beta = 3 \times 10^{-3}$ ), and the UV flux is relatively strong (with  $F_{UV} = 10^6$  erg cm $^{-2}$  s $^{-1}$ ), the magnetic fields almost completely suppresses the outflow, i.e., flow takes place only along a highly limited fraction of the field lines.

Comparison of Figures 1 and 2 shows that the geometry of the background field (due to the star) can play an important role in shaping planetary outflows. In this specific case, the background geometry of the split-monopole field (shown in Figure 2) acts to suppress the mass loss rate (recall that even aligned background fields suppress outflow rates relative to the field-free case). Although not shown in Figure 2, the flow at high latitudes shows time-variability. This departure from steady-state flow is observed in numerical simulations where the outflow has difficulty passing through the sonic point (Owen & Adams, 2014) and depends quite sensitively on the background magnetic field (Adams, 2011).

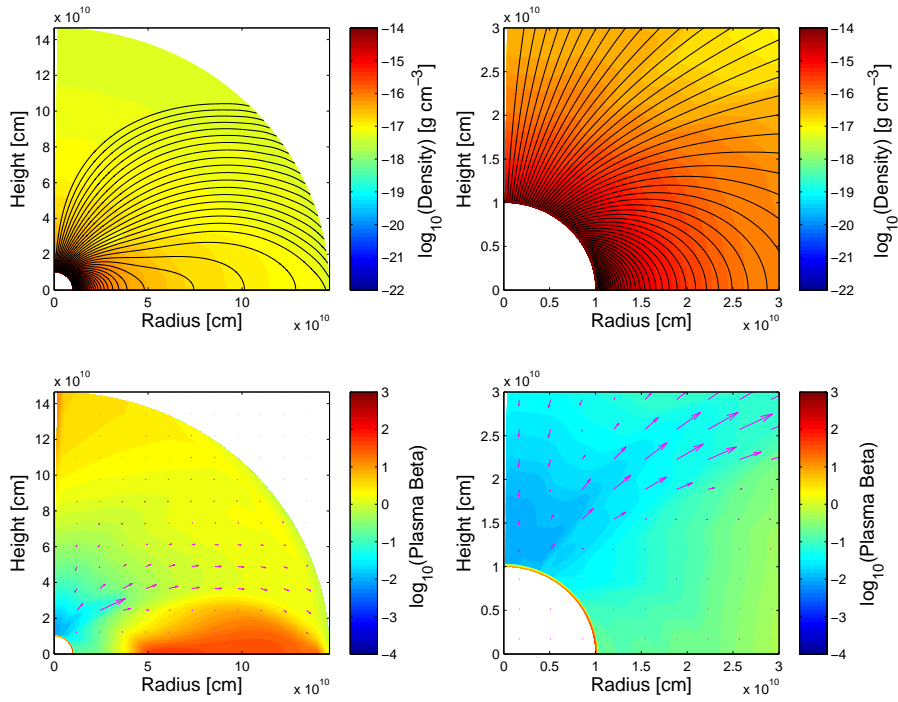


Figure 2.: *Simulation of planetary outflow where the stellar background field has a split monopole configuration. Here the stellar field points in the  $\hat{x}$  direction (in the coordinate system centered on the planet), whereas the magnetic dipole of the planet points in the  $\hat{z}$  direction. The planetary field  $B_P = 0.5$  gauss, the field strength ratio  $\beta = 3 \times 10^{-3}$ , and the stellar UV flux  $F_{UV} = 10^6 \text{ erg cm}^{-2} \text{ s}^{-1}$ .*

#### 4. Conclusion

This contribution reviews recent progress concerning magnetically controlled outflows from Hot Jupiters and presents results comparing different configurations for the background magnetic field due to the star. The following results emerge from this work:

[1] Planetary outflows are magnetically controlled. Even in the limiting case of relatively weak fields ( $B_P \sim 0.5$  gauss) and intense UV heating ( $F_{UV} = 10^6$  erg cm<sup>-2</sup> s<sup>-1</sup>) the magnetic field lines guide the flow.

[2] Magnetic fields act to suppress the mass outflow rates relative to the values obtained in the  $B \rightarrow 0$  limit (and relative to the energy-limited expression of equation [2]). As a rule, the outflow rates are suppressed by an order of magnitude.

[3] Magnetic fields change the geometry of the flow. Not all field lines are open and can support outflow. The fraction of open field lines is determined mostly by the background magnetic field structure, but also by thermal pressure opening up planetary field lines. In addition, magnetic fields suppress the transfer of heat to the night side of the planet and suppress outflow from that hemisphere.

[4] The manner in which the magnetic fields of the planet match onto the background environment, provided by the stellar magnetic field and the stellar wind, is important. The geometry of the background magnetic field affects the fraction of the planetary surface that supports open field lines and hence outflow (compare Figures 1 and 2).

*Acknowledgements.* We would like to thank the organizers of Cool Stars 18 for inviting this contribution. The numerical calculations were performed on the Sunnysvale cluster at CITA, which is funded by the Canada Foundation for Innovation. We are grateful for the hospitality of both CITA and the University of Michigan for visits that helped facilitate this collaboration.

#### References

- Adams, F. C. 2011, ApJ, 730, 27
- Adams, F. C., & Gregory, S. G. 2012, ApJ, 744, 55
- Baraffe, I., Alibert, Y., Chabrier, G., & Benz, W. 2006, A&A, 450, 1221
- Baraffe, I., Selsis, F., Chabrier, G., Barman, T. S., Allard, F., Hauschildt, P. H., & Lammer, H. 2004, A&A, 419, L13
- Batygin, K., & Stevenson, D. J. 2010, ApJ, 714, 238
- Eggleton, P. Kiseleva, L. & Hut, P. 1998 ApJ 499, 853
- Fabrycky, D. & Tremaine, S. 2007, ApJ, 669, 1289
- Fares, R., et al. 2010, MNRAS, 206, 407
- García Muñoz, A. 2007, Planet. Space Sci., 55, 1426
- Gregory, S. G., Jardine, M., Gray, C. G., & Donati, J.-F. 2010, Reports on Progress in Physics, 73, 126901

- Gregory, S. G. 2011, *Am. J. Phys.*, 79, 461
- Hayes, J. C., Norman, M. L., Fiedler, R. A., et al. 2006, *ApJS*, 165, 188
- Holmström, M., Ekenbäck, A., Selsis, F., Penz, T., Lammer, H., & Wurz, P. 2008, *Nature*, 451, 970
- Lai, D., Helling, Ch., & van den Heuvel, E.P.J. 2010, 721, 923
- Lammer, H., Selsis, F., Ribas, I., Guinan, E. F., Bauer, S. J., & Weiss, W. W. 2003, *ApJ*, 598, 121
- Lanza, A. F. 2008, *A&A*, 487, 1163
- Lanza, A. F. 2009, *A&A*, 505, 339
- Lecavelier des Etangs, A., Ehrenreich, D., Vidal-Madjar, A., Ballester, G. E., Désert, J.-M., Ferlet, R., Hebrard, G., Sing, D. K., Tchakoumegni, K.-O., & Udry, S. 2010, *A&A*, 514, 72
- Lin, D.N.C., Bodenheimer, P., & Richardson, D. C. 1996, *Nature*, 6575, 606
- Lissauer, J. J., & Stevenson, D. J. 2007, in *Protostars and Planets V*, eds. B. Reipurth, D. Jewitt, and K. Keil (Tucson: Univ. Arizona Press), p. 591
- Moorhead, A. V., & Adams, F. C. 2005, *Icarus*, 178, 517
- Murray-Clay, R. A., Chiang, E. I., & Murray, N. 2009, *ApJ*, 693, 23
- Owen, J. E., & Adams, F. C. 2014, *MNRAS*, in press, arXiv:1408.3636
- Owen, J. E., & Wu, Y. 2013, *ApJ*, 775, 105
- Papaloizou, J.C.B., & Terquem, C. 2006, *Rep. Prog. Phys.*, 69, 119
- Rasio, F., & Ford, E. B. 1996, *Science*, 274, 954
- Shkolnik, E., Walker, G.A.H., Bohlender, D. A., Gu, P.-G., & Kürster, M. 2005, *ApJ*, 622, 1075
- Shkolnik, E., Bohlender, D. A., Walker, G.A.H., Collier Cameron, A. 2008, *ApJ*, 676, 628
- Stone, J. M., & Norman, M. L. 1992, *ApJS*, 80, 753
- Stone, J. M., & Norman, M. L. 1992, *ApJS*, 80, 791
- Stone, J. M., & Proga, D. 2009, *ApJ*, 694, 205
- Trammell, G. B., Arras, P., & Li, Z.-Y. 2011, *ApJ*, 728, 152
- Trammell, G. B., Arras, P., & Li, Z.-Y. 2014, *ApJ*, 788, 161
- Vidal-Madjar, A., Lecavelier des Etangs, A., Désert, J.-M., Ballester, G. E., Ferlet, R., Hébrard, G., & Mayor, M. 2003, *Nature*, 422, 143
- Watson, A., Donahue, T., & Walker, J. 1981, *Icarus*, 48, 150
- Wu, Y. & Murray, N. 2003 *ApJ* 589, 605
- Yelle, R. V. 2004, *Icarus*, 170, 167